Student thesis series INES nr 448

Statistical Modelling of Permafrost Extent in the Circum-Arctic Region

Patricia Koch

2018

Department of

Physical Geography and Ecosystem Science

Lund University

Sölvegatan 12

S-223 62 Lund

Sweden

Patricia Koch (2018).
Statistical Modelling of Permafrost Extent in the Circum-Arctic Region
Statistisk modellering av permafrost i arktiska polarområden
Bachelor degree thesis, 15 credits in *Physical Geography and Ecosystem Analysis*
Department of Physical Geography and Ecosystem Science, Lund University

Level: Bachelor of Science (BSc)

Course duration: *March* 2018 until *June* 2018

Statistical Modelling of Permafrost Extent in the Circum-Arctic Region

---

Patricia Koch

Bachelor thesis, 15 credits, in *Physical Geography and Ecosystem Analysis*

Supervisor Paul Miller
Lund University

Exam committee:
Veiko Lehsten, Lund University
Vaughan Phillips, Lund University

Acknowledgements

I would like to thank my supervisor Paul Miller for continuous valuable advice, guidance in the search for suitable literature as well as providing the averages of the 30 years temperature data. Thank you as well to my examiners Veiko Lehsten and Vaughan Phillips for critical input. Furthermore, I am grateful for the feedback of my classmates Malin Ahlbäck and Franziska Weichert. I would also like to thank Geert Hensgens for aid with correlation functions in R and Mélanie Koch for the help with finding literature on engineering guidelines in Alpine permafrost regions. Special thanks to Francesco Pomati at Eawag Dübendorf for giving me the opportunity to learn about statistical modelling in R.

Abstract

Permafrost regions cover approximately a quarter of the Northern Hemisphere and thawing has been recorded in many different locations. The thawing process is likely to continue given that the Northern Latitudes will experience increased warming, which is known as the Arctic Amplification Factor. Changes in permafrost regions can cause changes in hydrology, biogeochemical cycles and ecosystems. Furthermore, infrastructure built on permafrost grounds such as cites and oil and gas pipelines are at high risk of collapse in the event of thawing. Additionally, there are large carbon pools stored in regions of frozen ground and release of carbon dioxide and methane could enhance the effect of global warming. While decrease in permafrost and its hazards have widely been recognized there is uncertainty about the extent of loss in permafrost area under different warming scenarios suggested by the IPCC. Models differ by their application so that global models are generally process-based and models in mountain areas often use statistical models. A previous study found a strong correlation between mean annual air temperature and current permafrost extent. This thesis investigates the relationship between growing and freezing degree days, seasonality and soil organic carbon content with regard to current permafrost extent and predicts permafrost loss for the RCP4.5 scenario. All variables are expected to show better or equal correlation coefficients as the mean annual air temperature as they give a more precise indication of the freezing conditions, which is supported by findings of previous local studies. The results show that none of the variables are a better indicator for permafrost. However, the predicted loss of permafrost by growing degree days with base temperature 5°C falls within the confidence interval of the permafrost-mean annual air temperature prediction.

Key words: permafrost, soil organic carbon, growing degree days, statistical modelling

Contents

List of Figures

List of Tables

1. Introduction

Permafrost, defined as ground that is frozen for two years or longer (NSIDC, 2018), covers about 25% of the Northern Hemisphere (Zhang et al. 2008). Global warming trends are more pronounced in the Northern Latitudes (Serreze et al. 2000) which alters the risk of permafrost soils thawing. This process has already been occurring in the past decades, as many in situ observations show (for example Serreze et al. 2000; Osterkamp 2005; Åkerman and Johansson 2008).

Effects of thawing permafrost can lead to changes in biogeochemical cycling (Hodgkins et al. 2014), hydrology (Walvoord and Kurylyk 2016) and ecosystems (Jorgenson et al. 2001; Shur and Jorgenson 2007). Furthermore, the degradation of permafrost can lead to a change in the landscape through geomorphological formations such as thermokarst (the melting of ice content in the permafrost layer) which disrupts surface topology through forming (water filled) troughs (Serreze et al. 2000; Nelson et al. 2002).

Despite being sparsely populated, security of infrastructure in the Northern Latitudes are of great importance since some cities and many oil and gas bases are located and built entirely on permafrost soils (Anisimov and Reneva 2006; Shiklomanov and Nelson 2013; Wang et al. 2016). Many of these regions are already facing damage to urban areas at a high cost such as damage to public infrastructure caused by melting permafrost (for example Canadian Broadcasting Corporation (CBC) 2017). Apart from construction issues, thawing permafrost releases carbon in form of carbon dioxide (CO_2) and methane (CH_4) from large carbon pools in the permafrost soils into the atmosphere (Schuur et al. 2015). This will likely enhance global warming and lead to further changes in the ecosystems (Schuur et al. 2008). While these changes have been widely recognised by science and political bodies alike, models differ in the magnitude of the predicted changes (Slater and Lawrence 2013). These models have taken several approaches to predict future permafrost extent depending on the region and application of the predictions (see Chapter 2.3). Scientific studies focus on local, regional and global modelling approaches that mostly apply physical formulae of e.g. heat transfer in soils or statistical approaches in areas with high spatial variability in permafrost (Riseborough et al. 2008). Aside from science, the field of engineering seeks to predict construction risks for regions with both permafrost and seasonally frozen soils (Bommer et al. 2009; Government of the Northwest Territories 2010). Data for these interactions can either be modelled or taken from e.g. borehole measurements or records from meteorological stations (Smith et al. 2010). Although measurement data is very reliable, it is very expensive and sometimes difficult to collect (Gruber and Haeberli 2009; Smith and Brown 2009) which is why modelled variables are used.

Comparing both single and combined variables with permafrost extent has shown strong correlations with permafrost (for example Riseborough et al. 2008). The use of multiple variables in models are commonly referred to as ‘multiple-criteria modelling’ (Etzelmüller et al. 2006) or ‘statistical-empirical modelling’ (Hoelzle et al. 2001) and are in particular frequently used in mountain permafrost regions (Riseborough et al. 2008).

A global study by Chadburn et al. (2017) found that mean annual air temperature (MAAT) is a good indicator of pan-arctic permafrost grouped in categories of permafrost content per volume of ground as suggested (Brown et al. 1997). Therefore, MAAT could be used to model the future extent of permafrost under increased temperatures that are predicted in the climate scenarios of the Intergovernmental Panel on Climate Change (IPCC) (Collins et al. 2013). Despite the strong correlation, MAAT is not solely responsible for the presence of permafrost as freezing conditions are dependent on many other factors (Smith and Riseborough 2002). Local studies have shown that air temperature-related indices are a more precise measure of permafrost and active layer depth (for example Åkerman and Johansson 2008). These indices include e.g. growing degree days (GDD) or freezing degree days (FDD) (also referred to as a thawing respectively freezing index) which have been incorporated in many established process-based models for permafrost predictions (Riseborough et al. 2008). The advantage of these indices is that they give a good estimation of warming and cooling intensities, which is often also approximated by seasonality.

1.1. Aim

The aim of this thesis is to examine the relationship between permafrost, categorized in percentage per area as determined by Brown (1997), and several climatic indices related to air temperature as well as the soil organic carbon content. In a second step variables with a significant relationship will be used to predict future permafrost distributions for warming of 1.5°C as suggested by the RCP4.5 scenario of the IPCC (Collins et al. 2013) while taking into account the Arctic amplification factor (Serreze et al. 2009).

This will be achieved by testing correlations between permafrost fractions and the variables:

1. **Thawing degree days** with base temperature **5°C** (cumulative sum of degree days above 5°C)
2. **Thawing degree days** with base temperature **0°C** (cumulative sum of degree days above 0°C)
3. **Freezing degree days** with base temperature 0°C (cumulative sum of degree days below 0 °C)
4. **Seasonality** (standard deviation of difference between the maximum temperature of the warmest month and the minimum temperature of the coldest month multiplied by 100)
5. **Soil organic carbon content** (soil organic carbon content in kg per m^{-2} from 0m to 3m depth)

The hypothesis is that all variables show a stronger correlation with the permafrost fractions than the MAAT and that they result in a similar loss in area under the projected warming. The geographic extent chosen is -180° W, 180° E, 40°N, 90°N to ensure that high latitudes and larger mountain regions are included.

2. Background

2.1. What is permafrost

The term permafrost defines the ground layer that is frozen continuously for at least two years (NSIDC, 2018). Permafrost regions can be found in polar and mountainous regions in both hemispheres (Gruber 2012) and are closely related to the presence of peatlands (Tarnocai et al. 2009). Peat has favorable heat conductivity properties protecting permafrost from summer heat inflow and cooling in winter months (Osterkamp and Burn 2015). Permafrost is most commonly grouped into the following categories suggested by Brown et al. (1997): Continuous (91-100% of area), discontinuous (51-90% of area), sporadic (11-50%) and isolated patches (0-10%). Furthermore, a distinction can be made between different amounts on ground ice content (grouped in high, medium and low), which is defined as the amount of visible ice in the uppermost 5 to 10 meters of the ground (Brown et al. 1997). Above the permafrost lies the *active layer* which undergoes seasonal thaw cycles and in which plant growth can take place (Serreze et al. 2000). Permafrost thawing has been recorded along with active layer thickening (Anisimov and Nelson 1996; Smith and Brown 2009). Therefore, active layer depth is often used as a proxy for permafrost in simple models (Riseborough et al. 2008). Many studies have shown a decrease in permafrost and a deepening of the active layer due to a warming climate (for example Åkerman and Johansson 2008; Bockheim et al. 2013).

2.2 Factors that influence presence of permafrost

There are numerous factors that influence the presence of permafrost whereas these factors also favor ground freezing. Permafrost in all regions is influenced by climatic variables and varies on local scales by topographic and physical factors (Osterkamp 2005). Many parameters, for example soil temperature, snow cover, aspect, elevation, albedo, soil composition, thermal conductivity, proximity to larger water bodies and vegetation type determine the presence of permafrost (Bommer et al. 2009; Donnell et al. 2010). The number of parameters that have to be included for predicting permafrost extent depends on the field of application. High resolution data and a large number of parameters are in particular needed in mountain areas where for example the aspect of the slope is a crucial indicator of the presence of permafrost (Gruber and Haeberli 2009). South facing slopes e.g. contain almost no permafrost despite favourable climatic conditions (Bommer et al. 2009). The different applications will be discussed later in Chapter 2.3. of this thesis.

2.1.1. Climatic factors

2.2.1.1. Air temperature

The primary factor is air temperature, which influences many other parameters such as the temperature of the soil. Air temperature has been found to be a good delineation of the permafrost zone when averaged over a yearly timespan (Smith and Riseborough 2002; Osterkamp and Burn 2015). For quantifying temperature many different indices can be calculated such as seasonality (difference of temperature between winter and summer months) (Popova and Shmakin 2009), cumulative thawing and freezing degree days (Frauenfeld et al. 2007; Åkerman and Johansson 2008) as well as the air freezing index (Nelson and Outcalt 1987).

2.2.1.2. Ambient soil temperatures

Despite the definition of permafrost being the soil below a specific soil temperature, permafrost presence can vary under the same climatic conditions (Shur and Jorgenson 2007). Soil temperatures give more precise values for temperature changes in the ground and therefore give a clearer indication of the presence

and vulnerability of permafrost. Temperature in the ground generally increases with increasing depth (Osterkamp and Burn 2015). Ground temperature in permafrost regions can vary greatly as found by a study in Canada where mean annual ground temperature ranged from -0.3°C to -14.9°C (Derksen et al. (2012). Variation has also been detected in the European Alps where temperatures approximately range between 0°C and -3°C, although colder temperatures are possible in mountain regions (Bommer et al. 2009). Alternatively, remote sensing or modelling techniques can be used to estimate soil temperature (Shi et al. 2018). If there is no possibility for direct measurement different formulas and models have been developed to calculate temperature offset in the ground from air temperatures (Smith and Riseborough 1998; Smith and Riseborough 2002).

2.2.1.3. Snow cover and precipitation

Water availability plays an important role in the freezing process of soils (Nicolsky et al. 2009). If water is available in unfrozen state from e.g. precipitation, this water content can change the conductivity parameters and can enhance the chance of freezing when soil temperatures cool (Nicolsky et al. 2009). Water in form of snow cover acts as an interface between the atmosphere and the ground and has significant influence on meltwater and thermal insulation (Beniston et al. 2018). The exact effect of snow cover depends on the general climate of the location and the length and timing of the snow season, snow depth, seasonality of the snowfall and the permafrost category (Zhang 2005). Generally, both seasonal and permanent snow cover have an insulating and therefore warming effect on the ground (Zhang 2005). This has been found in observational approaches (Smith et al. 2010), modelling (Stieglitz et al. 2003) as well as in experimental studies where snow accumulation was compared plots of artificial accumulation of snow with help of snow fences (Johansson et al. 2013). Despite this, the presence of a glacier does not exclude the possibility of permafrost ground (Waller et al. 2012).

There are two instances in an annual cycle where snow can have a cooling effect on the ground: 1) At the beginning of the snow season when there is only a thin snow cover on the ground and ambient temperatures are still relatively high (Zhang 2005). 2) At the end of the snow season when a significant amount of the solar energy is consumed by the melting process (Zhang 2005). These occasions however do not have a big effect on the ground temperatures (Zhang 2005).

2.2.2 Topography

Topographical parameters are important especially for mountain permafrost due to the high spatial variability on mountain slopes. Since the thesis focuses on a modelling approach covering the circum-arctic region these factors will not be dealt with in depth since the resolution of the datasets used is not precise enough for a sound statement in mountain areas. Therefore, the following description is a simplification of the conditions used to determine permafrost in these areas.

The most important indicator of permafrost in mountainous areas is elevation as it is closely related to air temperature. In Switzerland, for example, 2200 m.a.s.l. is given as a general indication in construction guidelines of elevation where permafrost is present (Bommer et al. 2009). However all topography-related factors such as aspect, slope, curvature and roughness influence the formation of permafrost in mountain areas (Gruber and Haeberli 2009) have to be taken into account when estimating permafrost content.

2.2.3. Heat transfer

Given favorable terrain and climatic conditions, freezing sensitivity and therefore permafrost formation ultimately depends on the ability of heat transfer to depth in the respective soil type. Generally a steep vertical temperature gradient is detected in all permafrost soils in which temperature increases with depth (Osterkamp and Burn 2015). Surface air temperature variations can affect soil temperatures to a depth of 5-6m (Williams and Gold 1976). Heat transfer is determined by the following physical parameters: Volumetric heat capacity (C), thermal conductivity (K), latent heat (the heat required to freeze or thaw a unit volume of frozen soil) (Williams and Gold 1976). These are closely connected to climatic inputs such as water availability so that a higher water content causes a higher thermal conductivity and heat capacity e.g. (Williams and Gold 1976). The aforementioned physical factors are also influenced by different

geological characteristics of the soil such as particle size (i.e. the content of e.g. sand, silt etc.) (Government of the North West Territories 2010), organic matter content, as well as plasticity, mineralogy and density (Schweizerischer Verband der Strassen- und Verkehrsfachleute (VSS) 2001). To estimate sensitivity of thawing in frozen ground air content, ice and water availability as well as bedrock type can be used (Bommer et al. 2009).

2.2.4. Vegetation

In a warming climate vegetation is expected to increase as both modelling, experimental and observational approaches show(Harsch et al. 2009; Natali et al. 2012; Pearson et al. 2013). These changes for example include increased greening (Xu et al. 2013), shift in species class (Pearson et al. 2013), advancing treelines (Harsch et al. 2009) or shrubification of the tundra (Zhang et al. 2013). Vegetation interactions and their effect on ground thermal conditions are connected to several different processes such as snowmelt, snow trapping, shading, solar radiation and water availability (Callaghan et al. 2011). It has been found that absence of vegetation leads to more direct thermal response of the ground towards atmospheric changes (Woo 2012)**.** When vegetation is present the degree of insulation widely differs between the vegetation types. Mosses and lichens e.g. have a high porosity and therefore infiltration of water is more pronounced than in other plant types (Woo 2012). In forests the leaf area index (LAI) is directly related to radiation and therefore also influences ground temperatures (Woo 2012). Additionally, the age of the forest and seasonal phenology influences transpiration (Woo 2012).

2.3. Measuring and estimating permafrost

2.3.1. Local scale and Engineering applications

For scientific studies on local scales and geotechnical site assessment in engineering many different measuring techniques exist to determine ground and climate conditions on site. However little long term monitoring data about decrease in permafrost due to changing climate is found (Anisimov and Reneva 2006).

Factors that determine a suitable construction ground could e.g. include topography, spatial and temporal snow cover, air temperature, radiation, surface properties, soil properties (e.g. heat conduction), hydrology (influence of flowing water and large water bodies), glaciers (possibly no permafrost) and the detection of ground ice within the permafrost are used for assessment for a suitable building ground and the calculation of risk resulting from frost damages (Bommer et al. 2009).

2.3.2. Modelling permafrost

Models mostly use interpolated point data of climate model output to predict climatic changes over a large geographic area (Riseborough et al. 2008). The main advantage of making large scale predictions is to give a better overview for global warming scenarios. For all spatial scales there are two main types of models we can distinguish: Simple models looking at relationships between variables and more complex process-based models (Riseborough et al. 2008). The latter incorporate dynamic parameters of (modelled) variables (see Chapter 2.2) (Riseborough et al. 2008). Process-based models examine the thermal state of the ground based on well-established physical principles of heat transfer (Riseborough et al. 2008). Their main focus lies on temporal, thermal and spatial criteria (Riseborough et al. 2008). Essentially process-based models are approximating the interaction between the ground/soil column and atmosphere by taking into account the cooling respectively warming intensity as well as the potential of the ground to transfer heat (Smith and Riseborough 1996; Osterkamp and Romanovsky 1997). There are a set of widely used process-based models such as the Stefan solution (calculating the moving freezing front with degree days, latent heat and conductivity), the Kudryavtsev solution (maximum annual depth of freezing/thawing) and the TTOP model (temperature at the top of the permafrost) (Riseborough et al. 2008). Furthermore, there are so called ‘numerical’ approaches to solving the equations of heat and moisture transfer in soils and snow in which many more soil parameters and properties can be included and where the ground temperature is calculated at every time step depending on the conditions of the previous step (Riseborough et al. 2008). Accuracy of

all models can be validated with measured data which is compared to the model output (Harris et al. 2009). The most precise models that are currently available for climate modelling are coupled global climate models (CGCMs), which consist of 'fully coupled atmosphere, ocean, land, sea ice and often biogeochemical components' (Slater and Lawrence 2013).

2.3.3. Statistical modelling

Statistical modelling enables the detection of long-term trends of observations and often uses measured input data. This is especially often used in mountain permafrost regions as physical processes vary on a small scale (Riseborough et al. 2008). These models can e.g. be used in multi-criteria approaches that determine the probability of permafrost presence with given parameters (Etzelmüller et al. 2006). The accuracy can be tested with recorded permafrost maps, statistical validation tests such as Kendall's τ (Gruber and Hoelzle 2008), the area under the receiver-operating characteristics curve (AUROC) (Boeckli et al. 2012) or forward conditional procedure (Ridefelt et al. 2008). Statistical modelling has for example been employed by Ridefelt et al. (2008) to determine permafrost in the mountainous area of the Abisko region (Sweden) and Boeckli et al. (2012) to model entire mountain regions. Limitations for applying statistical modelling on global scales are data availability (Gruber 2012), the fact that models do not account for thermal inertia of the ground as well as the issue that there is no measure for heat flow between the measurement points (Riseborough et al. 2008). Despite often simplifying the encountered conditions statistical exploration of permafrost-relevant data can be useful to support the use of physical formulae and modelled input data in process-based modelling.

2.4. Variable descriptions

2.4.1. Mean annual air temperature (MAAT)

MAAT has been found to give a good indication for permafrost both as a continuous variable of the fraction of frozen ground in various studies including the determination of the categories suggested by (Brown et al. 1997) and estimation of active layer depths (Koven et al. 2013). This was confirmed for different scales such as in the global study by (Chadburn et al. 2017) and on local scales (Etzelmüller et al. 2006). Permafrost presence/absence however shows variations beyond MAAT differences (Harris et al. 2009). These variations can for example be connected to topography, snow or vegetation etc. (Donnell et al. 2010).

2.4.2.1 Freezing and thawing days

Growing degree days (GDD) (also called Thawing Degree Days, TDD) are defined as the cumulative sum of degree days above a defined base temperature. This index is often used in agronomy or plant science (Michigan State University Extension 2017) as well as in engineering, where it is mostly referred to as thawing index (Bommer et al. 2009). The base temperature can e.g. be the freezing point (0°C) or 5°C which is considered the minimum temperature required for plant growth (Government of Saskatchewan 2013). The formula for the GDD is as follows (modified from Cropwatch, University of Nebraska in Lincoln, 2015):

$$(1) \qquad GDD = \sum_{i=1}^{N_{Tmean}=366} T_{mean} - T_{base} \mid T_{mean} > T_{base}$$

Åkerman and Johansson (2008) found that along a transect in the Torneträsk region in Northern Sweden GDD gives a better correlation with active layer depth than MAAT. GDD have also shown to have a significant influence on gelifluction, nivation and mounding in periglacial regions in other parts of Northern Europe (Aalto et al. 2017).

Freezing degree days (FDD) represent the cumulative sum of degree days below the freezing point (0°C), which are most often employed in cryospheric research (Van Everdingen 2005; Frauenfeld et al. 2007). The FDD can be calculated with the following formula (modified from Frauenfeld et al. 2007):

$$(2) \qquad FDD = \sum_{i=1}^{N_{Tmean}=366} T_{base} - T_{mean} \mid T_{mean} < T_{base}$$

FDD can be used as an indicator for permafrost (Nelson and Outcalt 1987)and to determine freeze depth, respectively active layer depth (Frauenfeld 2004; Wu et al. 2011), and is frequently applied in freezing measurements in engineering (Schweizerischer Verband der Strassen- und Verkehrsfachleute (VSS) 2001; Government of the North West Terrotories 2010). Furthermore, a study has shown that FDD has a significant effect on cryoturbation in Northern Europe (Aalto et al. 2017). The FDD can either be based on daily or monthly temperatures (Frauenfeld et al. 2007). To account for a period of continuous freezing and the FDD are more correctly represented by calculating the cumulative sum for the winter months rather than over the timespan of an entire year (Frauenfeld et al. 2007). The reference temperatures are usually records of the past 30 years (Frauenfeld et al. 2007; Bommer et al. 2009).

2.4.2. Seasonality

Seasonality quantifies the extremes over an annual timespan and is calculated as the annual temperature range expressed as the difference between the maximum temperature of the warmest month and the minimum temperature of the coldest month (Xu and Hutchinson 2011). General ground temperature regimes in permafrost are also, to a certain depth, influenced by seasonality with an offset with increasing depth (Bommer et al. 2009). Mann and Park (1996) found that since global warming was more pronounced from 50° poleward in the winter season, seasonality will decrease in the face of climate change. In addition, several studies show a change in seasonality snow cover in the Alps (Beniston et al. 2018). Temperature seasonality has been found to be correlated with active layer depth across different landscapes in Western Siberia (Popova and Shmakin 2009) and therefore could potentially also be a useful indicator for permafrost. Despite the fact that changes in permafrost seem to occur on larger temporal scales than intra annual variations there might be a relationship between the categories based on the underlying connection of seasonality to water availability, snow season parameters and variations in ground heat.

2.4.3. Soil organic carbon (SOCC)

A critical point regarding permafrost thawing are the large organic carbon pools (~1700 Pg C) that are stored in in the soil of the Northern circumpolar permafrost zone (Schuur et al. 2013). In a warming environment carbon could leave the soil in the form of CO2 and CH4 emission (Anisimov 2007). This exchange can take place in the anaerobic pathway for methane and via both aerobic and anaerobic pathways for carbon dioxide (Schuur et al. 2015). Aerobic pathways mostly take place in upland ecosystems whereas anaerobic pathways dominate in lowland lakes and wetlands (Schuur et al. 2015). A consultation of several experts in the field by Schuur et al. (2013) concluded that between under RCP8.5 (highest emission scenario) 162 and 288 Pg C will be lost from the northern circumpolar permafrost zone by 2100. Detecting significant differences between the different permafrost categories could potentially reveal regions where carbon content is more vulnerable to climate change.

3. Materials and Methods

For the statistical analysis of the chosen variables, freely available datasets were used and analyzed in the statistical software RStudio. All datasets considered data points available in the extension of -180°E, 180°W, 40°N, 90°N on a WGS84 projection. The resolution was 0.5° for all datasets except for the seasonality variable (see Chapter 3.1 and 5.1). The extent was chosen based on availability of the Circum-Arctic Map of Permafrost and Ground Ice Conditions (Brown et al. 1997 via Pangaea. 2018) and includes major mountain areas outside the Arctic region. Valid land points were selected from the coordinate points of the SOCC dataset as this had the smallest amount of data points.

All datasets were opened in RStudio and joined in tables by matching coordinates and selecting only complete data rows. The dataset for carbon provided data for only 17880 grid cells and matched 17943 cells of the other variables. Therefore 17843 was chosen as the number of input cells for the statistical analysis.

Table 1: Number of land points (grid cells) with data. The originally intended extent (-180, 180, 40, 90 extent with 0.5° resolution) including ocean points was 72'000.

Variable	Valid land cells
MAAT, GDD, FDD	33765
Permafrost	23749
SOCC	17880
Total points in common	17843

3.1. Datasets

The Circum-Arctic Map for Permafrost and Ground Ice Conditions was published in 1997 by (Brown et al. 1997) and shows current permafrost fraction distributions (comprising data from 1960 to 1993 (Slater and Lawrence 2013)). The map (see Figure 1) was available as a download in the supplement to the online version of the paper by Chadburn et al. (2017) on website of Pangaea (2017). Units are given as fractions of permafrost per m^2 to 3m depth. These fractions per half coordinate were used as a reference permafrost distribution.

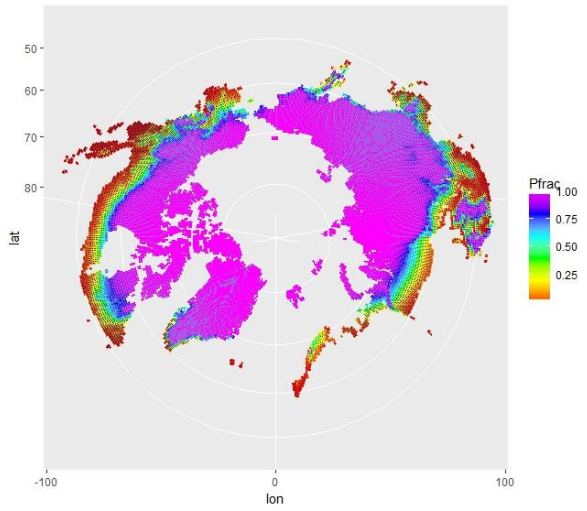

Figure 1: Circum-Arctic distribution of permafrost.

Daily average air temperatures (in degrees Kelvin) from the 1st of January 1979 to the 31st of December 1990 from the WATCH forcing dataset (Weedon et al., 2014, accessed via DataGURU, 2018) were used to calculate the growing degree days for T_{base} 5°C and 0°C as well as the freezing degree days (0°C). The temperatures per day were averaged over 11 years. The time period was chosen to be 20 years shorter than in the reference paper by Chadburn et al. (2017) with the intention to keep the processing size of the files at a minimum. The formulas used were identical to the ones mentioned in Chapter 2.4.2.1. Daily average temperatures were used to calculate GDD0 (see Figure 2), GDD5 (see Figure 3), FDD (see Figure 4) and MAAT (see Figure 5).

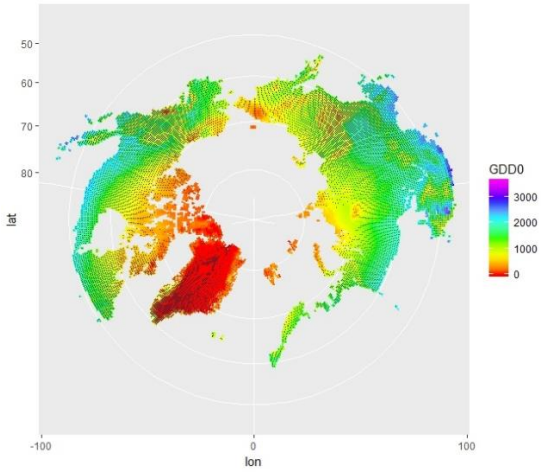

Figure 2: Circum-Arcitc distribution of GDD0.

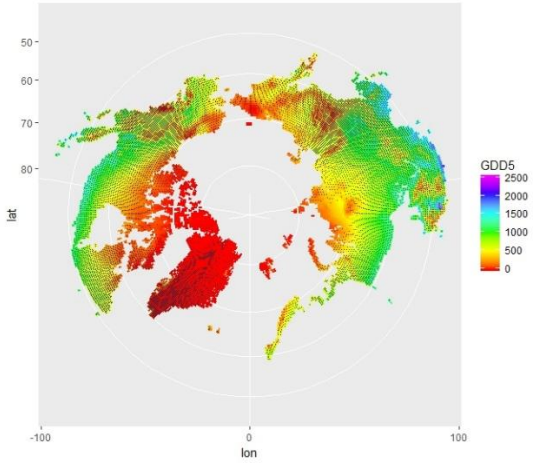

Figure 3: Circum-Arctic distribution of GDD5.

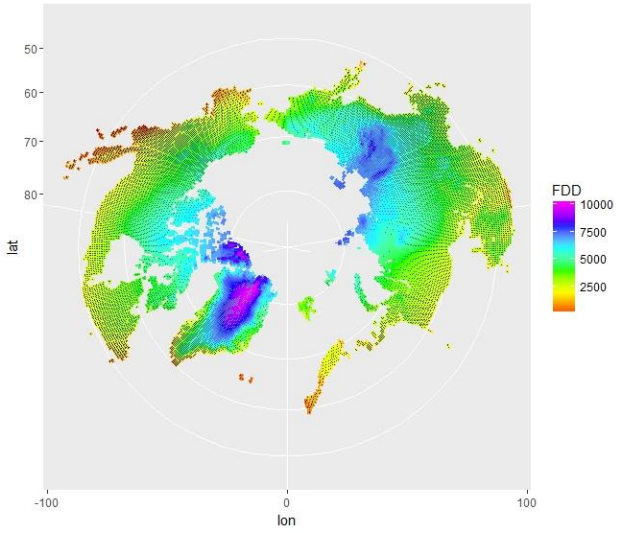

Figure 4: Circum-Arctic distribution of FDD.

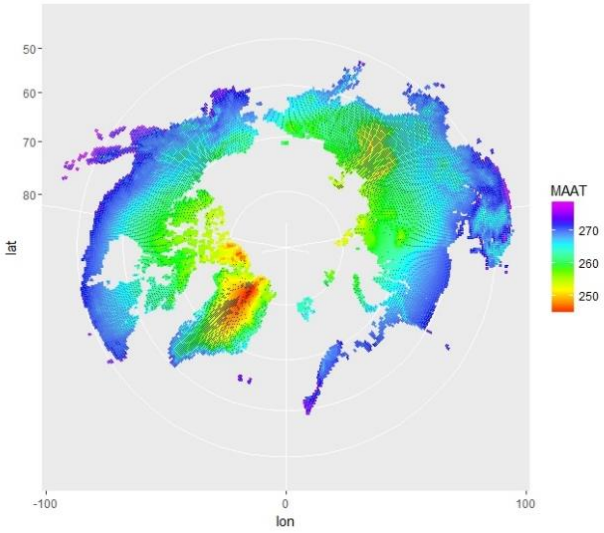

Figure 5: Circum-Arctic distribution of MAAT.

The dataset for seasonality was obtained from Bioclimatic Variables of the Worldclim dataset (Fick and Hijmans, 2017) at 10 minutes resolution, as this was the lowest resolution at which the dataset could be obtained. By combining all variables into the final table only matching coordinates to the 0.5° resolution were used (see Chapter 5.1 Limitations and Sources of Error). The variable chosen as a measure of

seasonality (see Figure 6) calculates the standard deviation of the weekly mean temperatures expressed as a percentage of the mean of those temperature multiplied by 100 (Worldclim, 2017; Xu and Hutchinson 2011).

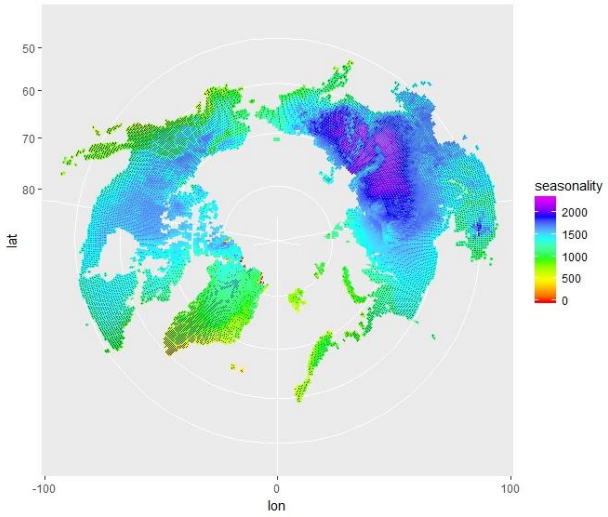

Figure 6: Circum-Arcitc distribution of seasonality.

Soil organic carbon data was obtained from the Northern Circumpolar Soil Database (Bolin Centre of Climate Research, 2018) which provides a 0.5° resolution map for soil, and SOCC maps in the circum-Arctic region. The interpolation spans across the area between the Circumarctic Active Layer Monitoring Network (CALM) (IPA, 2008) research stations and therefore does not fill the full extent of the studied map (-180, 180, 40, 90). The number of grid cells available was n=23749.
The variable selected from the dataset was the amount of soil organic carbon in kilogram per square meter. The data was available at four different depths: 0-30cm, 30-100 cm, 100-200cm, 200-300cm. The sum of all layers was calculated to obtain the total amount of carbon per coordinate (see Figure 7).

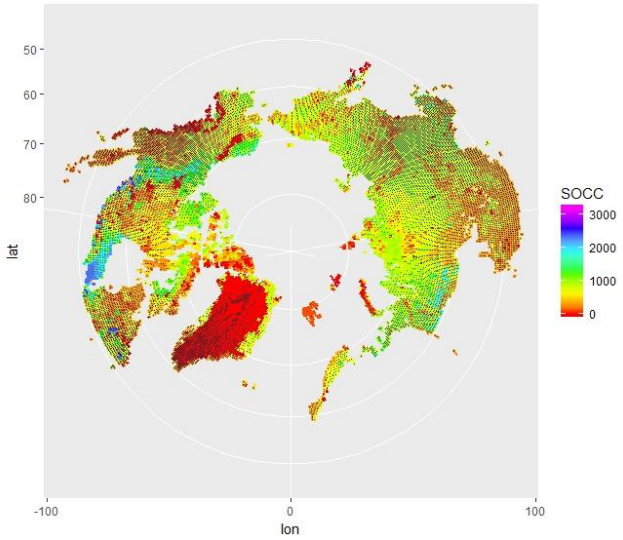

Figure 7: Circum-Arctic distribution of SOCC from 0 to 3m depth.

3.2 Analysis and Prediction

Each variable was analyzed as a continuous variable as well as grouped in 'continuous' , 'discontinuous', 'sporadic' and 'isolated patches' (see Chapter 1.1). Frequency distributions and different types of plots with the permafrost fractions versus the climate and soil variables were used to explore general behaviour of the variables. Correlation coefficients were calculated between each variable and the permafrost fraction with the *cor.test* function in RStudio using the Pearson correlation. Furthermore, the *cor* function (using Pearson's correlation coefficient) was used to create a correlation plot to visually represent the coefficients. Maps, basic statistics and distributions were examined and compared to the MAAT. For the prediction, due to the lack of time, only the 1.5°C (288.15 K) warming scenario was calculated for GDD5 and GDD0 the Arctic amplification factor was simplified to a multiplication factor 2 (variation in the study by Chadburn et al. (2017) ranged between 1.7987 and 2.6 per latitudinal category). To modify the GDD a value of 3 was added to every cell of the temperature dataset. This number is derived from Formula 3, which multiplies the average annual warming of 1.5°C (288.15 K) by 2, which is the Arctic Amplification Factor. Flowingly, the GDD was recalculated as in Formulas 1 and 2.

$$\Delta T = 2*1.5 = 3 \quad (3)$$

1st and 3rd quartiles (equivalent to 25% and 75% of the dataset) were considered as thresholds for delineating the permafrost categories. As these sometimes overlapped, the change in permafrost cover was calculated as the number of grid points falling into the respective category. The sum of these counts was subtracted from the present day permafrost cell counts to obtain the net loss permafrost area. The area was calculated with Formula 4, whereas e grid cell.

$$A_{Pfrac} = \Delta n_{Pfrac} * \left(\frac{110.57}{2}\right)^2 \quad (4)$$

Whereas Δn_{Pfrac} is the count of the net loss of permafrost fraction (as a continuous variable) and the multiplication factor is the length of 1° in km (divided by 2 for obtaining 0.5° for the given resolution) and squared to calculate the surface in km^2. This result could be compared to the estimation of the 1.5°C warming scenario suggested by Chadburn et al. (2017).

4. Results

From the maps showing the spatial distributions (see Chapter 3.1) of the variables it can be seen that there is a large variation of the number of degree days in GDD0 and the FDD than GDD5. Difference in the pattern between GDD and FDD is found in Siberia. MAAT shows strong latitudinal delineation. Seasonality generally follows a similar pattern as FDD and GDD but does not show detailed differences between the regions except for north-east Russia and the Western coast of North America. Soil organic carbon contents vary widely per geographic region and no apparent latitudinal or topographical pattern can be recognized.

The scatterplots show a wide range of values of the variables corresponding to one unit of permafrost fraction (see Figure 8). The clearest relationships is seen in FDD while GDD0 and GDD5 show general trends. Seasonality and SOCC do not show and specific relationship to permafrost fraction. The scatterplot of MAAT (Figure 9) shows a clearest correlation.

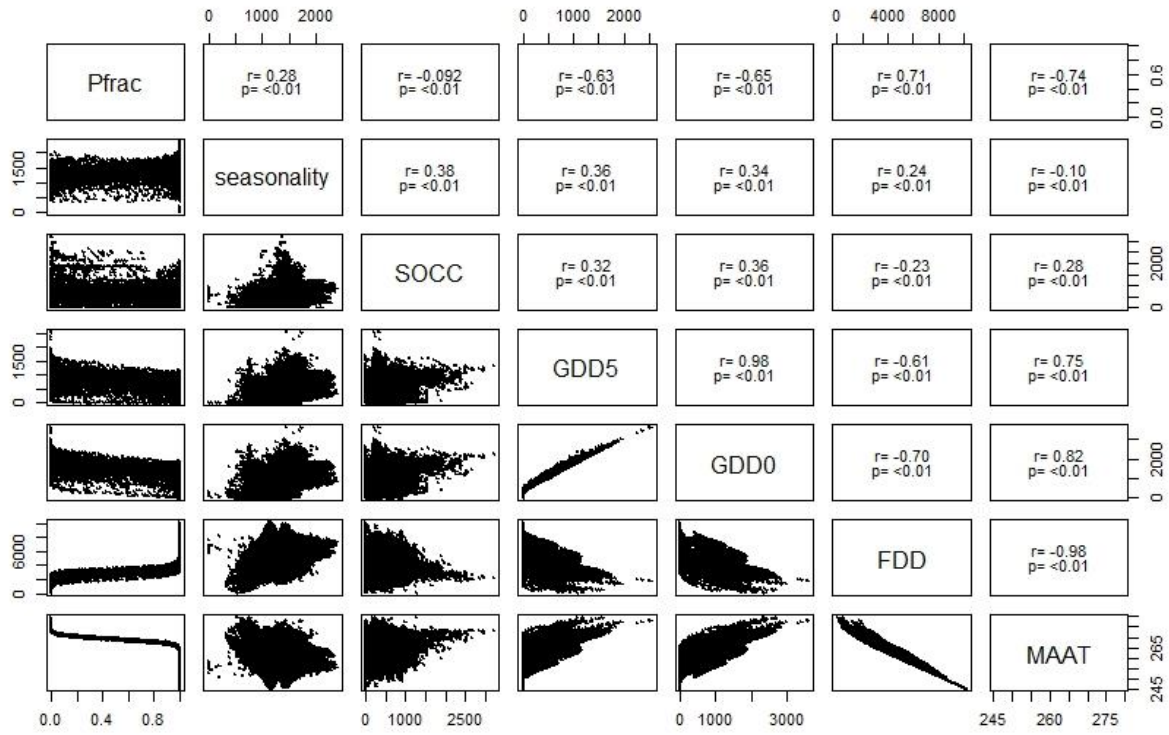

Figure 8: Scatterplots of variables permafrost fraction, seasonality, GDD0, GDD5, FDD, SOCC and seasonality. The clearest relationship can be seen between permafrost fraction and FDD. The two GDD variables are, as expected, strongly correlated.

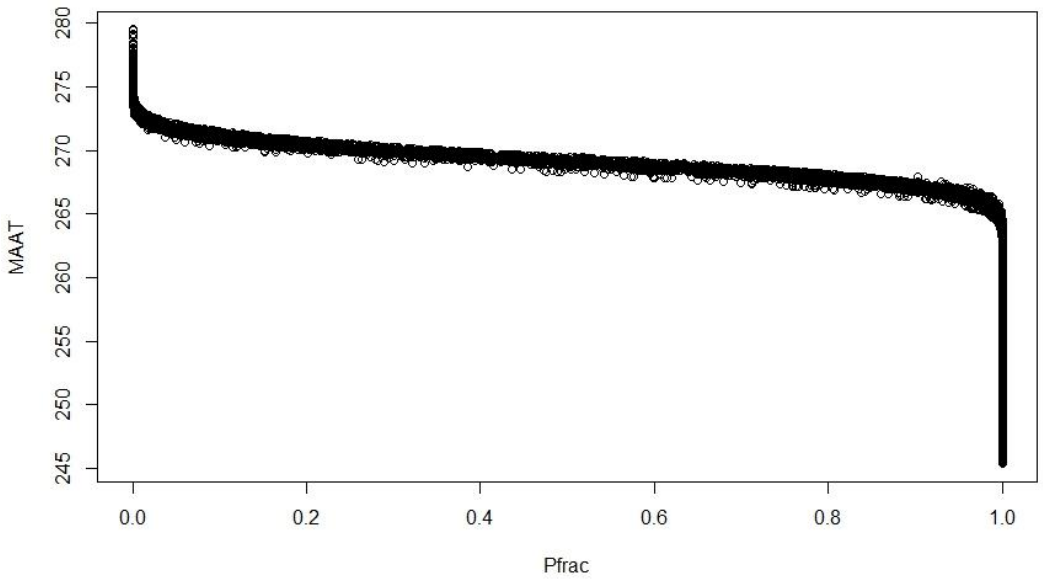

Figure 9: Relationship between permafrost fraction and MAAT. The plot shows a clearer correlation than the other tested variables.

The boxplots show that all tested variables have a wide range of values within the same permafrost category. GDD0 (see Figure 10) and GDD0 (see Figure 11) show that that certain permafrost categories differ significantly in relation to growing degree days but also show a large spread. The largest spread is found in the isolated permfrost for all variables except for the FDD (see Figure 12) and MAAT (see Figure 13), where the continuous permafrost has the largest spread. From the tested variables none gave a better estimate of the permafrost fractions than the one presented by Chadburn et al. (2017). Seasonality (see Figure 13) did not show a specific trend related to the permafrost categories.

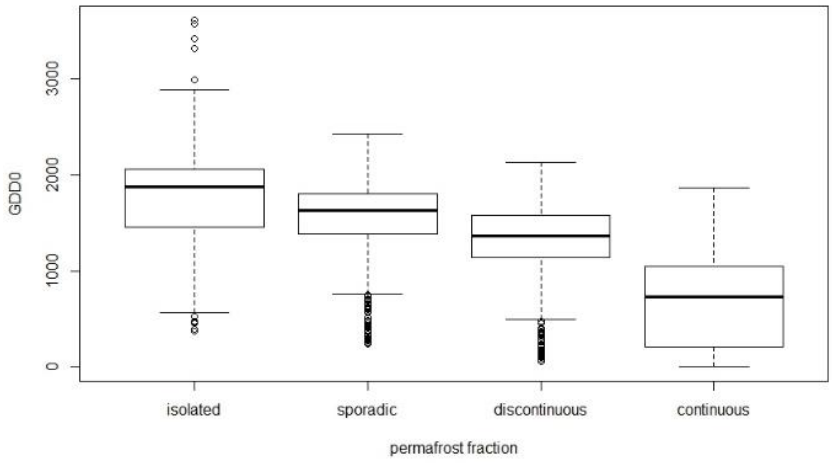

Figure 10: GDD0 values per permafrost category.

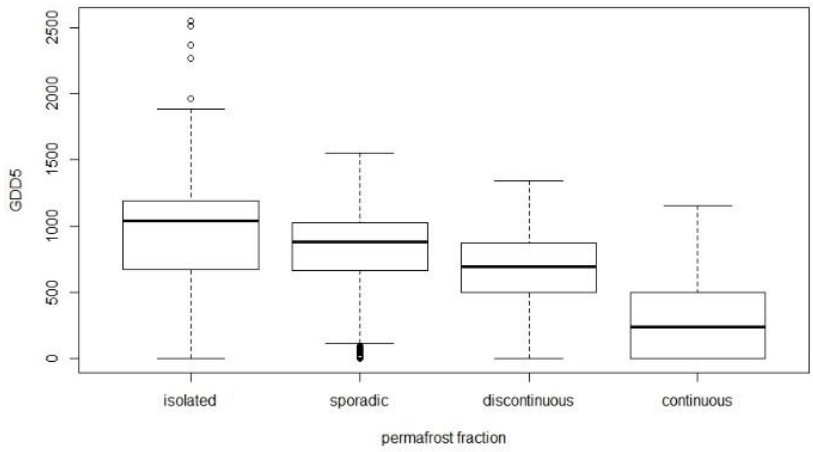

Figure 3:GDD5 values per permafrost category.

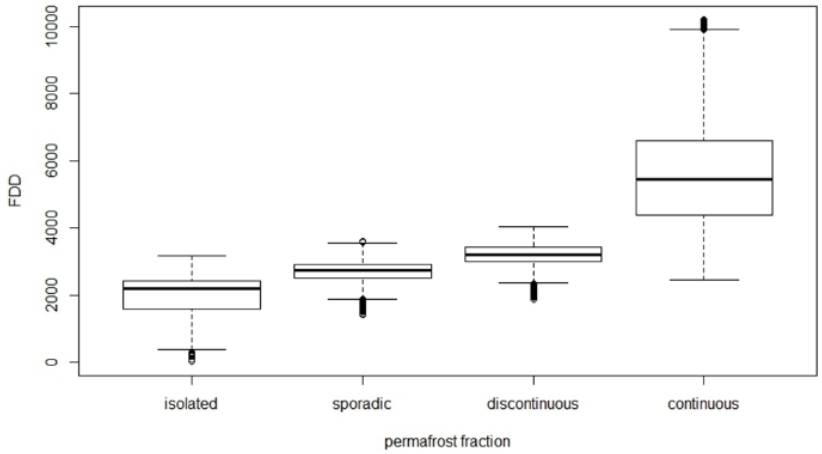

Figure 4: FDD values per permafrost category.

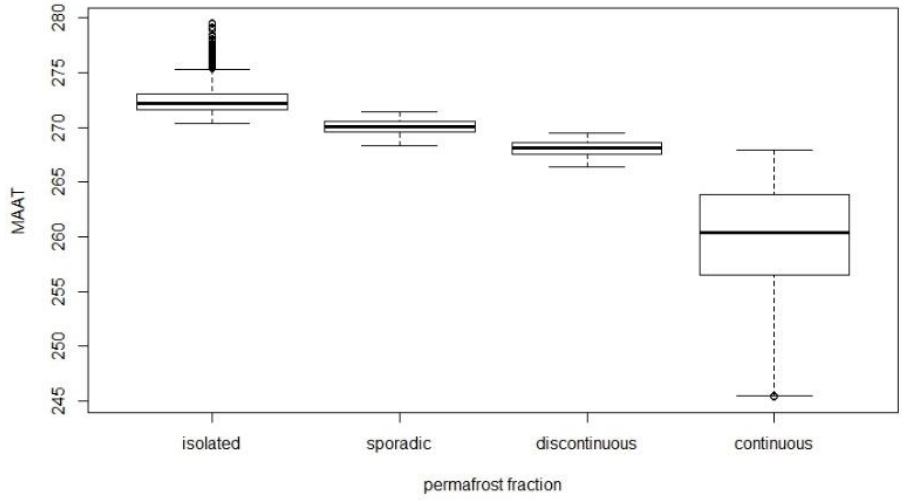

Figure 5: MAAT values per permafrost category.

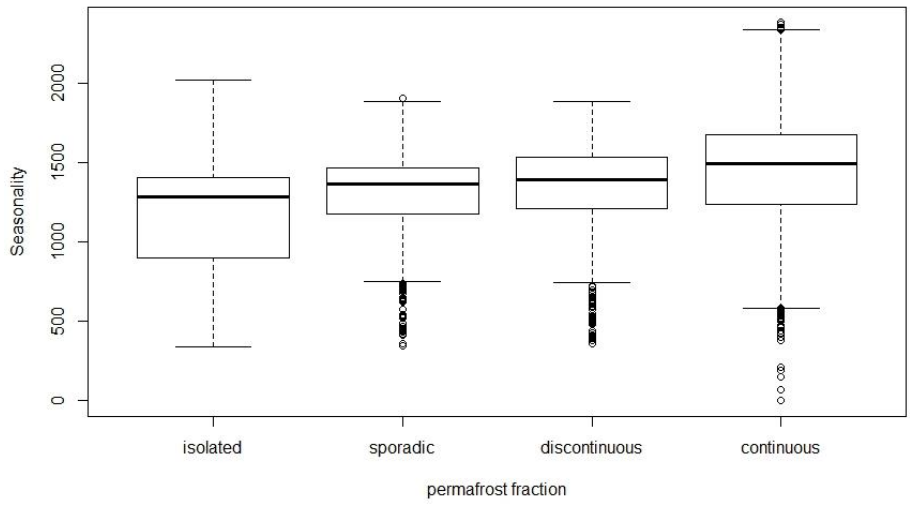

Figure 6: Seasonality values per permafrost category.

Table 2 and 3 show the values for the mean and 1st and 3rd quartile (see limits of the boxes in Figures 11 and 12). Freezing degree days show a similar pattern as the MAAT however the variance for all categories is larger than in MAAT. As in the GDD0 the variance is biggest in the isolated permafrost.

Table 2. Mean, 1st and 3rd quartile for GDD0 per permafrost category.

Variable	**Mean GDD0 original**	**1st quartile**	**3rd quartile**
continuous	688.83	205.50	1051.80
discontinuous	1334.37	1142.49	1582.69
sporadic	1567.83	1376.00	1799.80
isolated	1785.61	1455.90	2055.80

Table 3: Mean, 1st and 3rd quartile for GDD5 per category.

Variable	**Mean GDD5 original**	**1st quartile**	**3rd quartile**
continuous	300.86	0.40	500.49
discontinuous	673.44	691.70	872.30
sporadic	831.33	661.70	1027.60
isolated	958.65	672.22	1186.90

SOCC showed almost no variation between the permafrost categories (see Figure 15) and a rather large variation within each category. The highest SOCC was found in continuous permafrost, which is the largest category of the entire permafrost area covered.

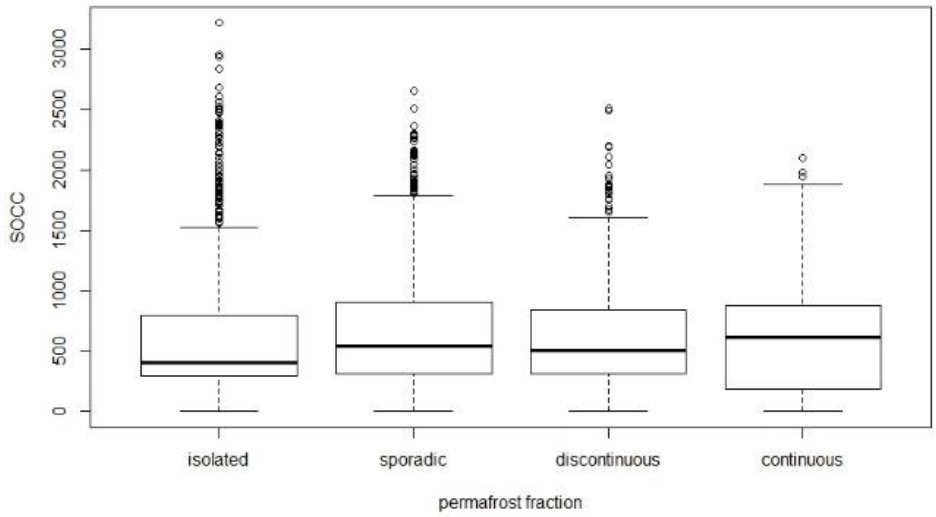

Figure 7: SOCC values per permafrost category.

Pearson correlation coefficients (see Table 4) show a small difference between the coefficients for MAAT and FDD. A comparison of all variables can be seen in Figure 16 which represents the Pearson correlation coefficients between the variable pairs.

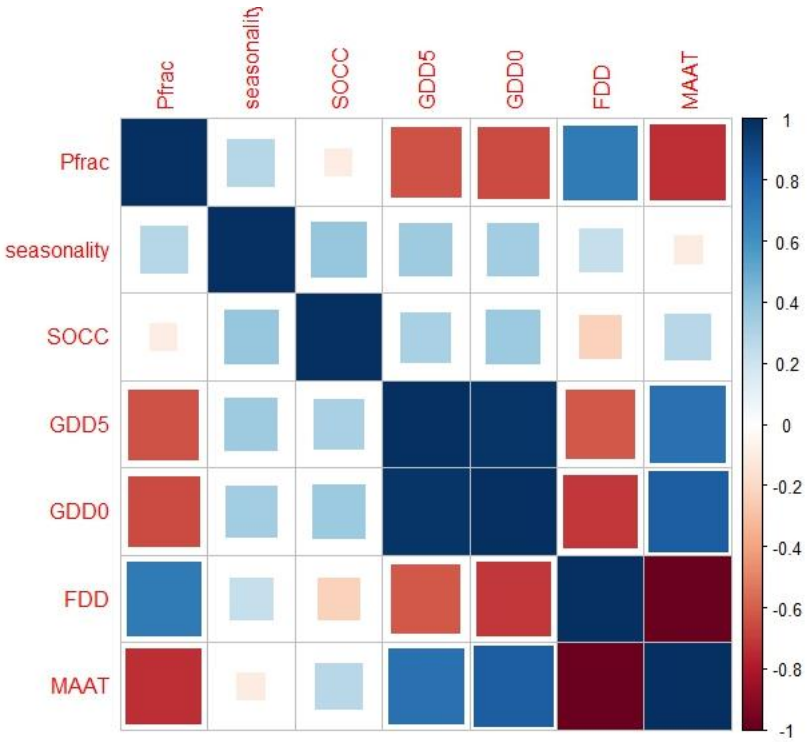

Figure 8: Correlation plot of different Pearson correlation coefficients of all variable pairs. The strongest correlation when looking at permafrost fractions are seen between MAAT as found by Chadburn et al. (2017) and FDD.

4.1 Predictions

Permafrost loss calculated for a RCP4.5 scenario of 1.5°C (Collins et al. 2013) warming would lead to a loss of 5.7 Mio. km^2 (~10.0% loss of the current permafrost) when using GDD0 and 4.4 Mio. km^2 (~7.8% loss) when using GDD5 (see Table 5).

Table 4: Loss of permafrost ground in units of cell numbers (number of coordinate points) and in square kilometers.

	Continuous	**Discontinuous**	**Sporadic**	**Isolated**	**Total**	**Thawed area [km^2]**
Current	12384	1988	1872	1807	18051	
GDD0 +1.5°C	3875	4035	3472	4816	16198	5'663'567
GDD5 +1.5°C	3984	2393	4434	5805	16616	4'385'979

5. Discussion

For a large scale study area distributions of different permafrost-relevant factors show that none of the tested variables is likely to give a better indication of permafrost presence than MAAT as found by Chadburn et al. (2017). This is consistent for all four permafrost categories. No significant relationship was found between SOCC and different categories of permafrost. The predicted loss of permafrost area in the event of a global warming of 1.5 °C is ~4.4 Mio km^2 using the GDD5-permafrost relationship and ~5.7 Mio km^2 for GDD0. The predicted area under GDD5 falls into the 2σ confidence interval of the result suggested by (Chadburn et al. 2017).

While MAAT is generally considered to be a good indicator of the permafrost categories suggested by (Brown et al. 1997) additional factors are needed to determine permafrost presence (Harris et al. 2009; Donnell et al. 2010). GDD as well as seasonality have proven to be good indicators in local or regional studies (Åkerman and Johansson 2008; Popova and Shmakin 2009) but have hardly been used for more global comparisons. Frauenfeld et al. (2007) suggest that the accuracy of both freezing and thawing degrees might differ since in shoulder seasons temperatures fluctuate around 0°C and therefore might give a biased result. This however is more pronounced if monthly air temperatures are used to calculated the FDD (Frauenfeld et al. 2007). Comparing correlation coefficients and frequency distributions shows that FDD has a similar accuracy as MAAT. However, FDD values within the categories have a wider interquartile range, especially for the continuous permafrost category. Additionally, there are many outliers in all other categories. Potentially both, FDD and MAAT, could be used for predictions of future climate. GDD0 does not show a comparable result to MAAT in the correlation but gives a higher correlation coefficient than GDD5. This could indicate that the cooling intensity is the most crucial determinant for permafrost occurrence on the circum-arctic scale rather than warming factors. This has been observed in permafrost decrease in Alaska where the decrease could mostly be explained by warming temperatures in winter (Osterkamp 2005).

Seasonality shows no trend towards a particular permafrost fractions, which is most likely because seasonality acts on an intra-annual scale, which is too small to influence the presence of permafrost. When considering the close the relationship between MAAT and seasonality it is also important to note that identical MAAT values in different these could be underlain by widely differing seasonality values. In addition, seasonality possibly has higher geographic variability than the resolution used.

Since many of the variables have performed better in local experiments the resolution of the used datasets could be seen as a limitation of our study (see Chapter 5.1). Another explanation for the performance of the variables could be that they are more crucial for susceptibility of thawing in permafrost rather than a good indicator of present conditions as many of the indices are used in engineering to estimate the risk of thawing (Schweizerischer Verband der Strassen- und Verkehrsfachleute (VSS) 2001; Bommer et al. 2009). MAAT

on a large spatial scale with low spatial resolution is a good indicator for permafrost, this can be supported by that fact that it is also strongly correlated with latitude.

The predicted surface can be compared to result of Chadburn et al. (2017) who found a 4.8 km^2 loss under RCP4.5 with a 2σ = +2.0/-2.2 uncertainty. The limits of uncertainty represent the upper and the lower curve of the initial relationship of the MAAT with the permafrost fractions. This was considered equivalent to the limit of two standard deviations (2σ). The prediction of both GDDs underestimates the area suggested by Chadburn et al. (2017) but GDD5 falls within the limits of the curve of the MAAT-permafrost fraction relationship. GDD0 underestimates the total loss but gives a closer value to the predicted loss by Chadburn et al. (2017) than GDD5, which falls into the upper limit of the confidence interval.

The mean values for SOCC range between 555 kg m^{-2} (continuous permafrost) and 686 kg m^{-2} (sporadic permafrost) and for the median between 396 kg m^{-3} (isolated) and 615 kg m^{-3} (continuous). This shows that no particular category has an association with significantly high SOCC. This is consistent with visual analysis when comparing the Circum-Arctic Map of Permafrost (Brown et al. 1997) with the Northern Circumpolar Map of Soil Carbon (see Figure 7). These results might seem positive but must be interpreted with caution and should be compared to SOCC of soils in lower latitudes that are less prone to warming.

Further research could focus on the same variables using a higher map resolution or relate the FDD, GDD and seasonality to the degree of change that is predicted or measured per fraction. Another essential variable that could be included would be water availability derived from measurements of precipitation.

5.1 Limitations and sources of error

The largest limitation is likely the 0.5° resolution of the dataset. While this was the only resolution that could be found for the permafrost map and corresponds to the resolution in the paper by Chadburn et al. (2017) it might be generalizing many factors that affect presence of permafrost. Most importantly this affects mountain regions (Gruber and Haeberli 2009; Chadburn et al. 2017) but also holds true for other regions with large spatial variation (Slater and Lawrence 2013). Given the background of the local studies and generally better accuracy for higher resolution, it is possible that there would have been stronger correlations between the variables and the permafrost fractions. Technical uncertainties are concerning the statistical tests used as there seemed to be discrepancies between different correlation tests in R despite using the same correlation statistic.

Making multiple predictions of permafrost loss per degree of global warming was not possible given the limited time available, the non-linear relationship detected between the variables as well as the comparatively worse performance in distribution, correlation coefficients and spread. Ideally, a fitted function for the given variables would be needed to test the correlation between the variables. Despite the attempt to fit several common distributions to the datasets for the climate variables in each permafrost category, none showed an accurate fit. More time and theoretical knowledge would be required to make sound statements about a fitted function to the data.

6. Conclusion

For the given circum-Arctic permafrost dataset, none of the tested variables gave a better estimate of current permafrost fractions in the Northern Circum-Polar Region, which indicates that the null hypothesis cannot be rejected. This can partly be explained by the strong relationship found for MAAT but also by the resolution of the datasets used. Furthermore, no significant difference or trend could be detected between SOCC in different permafrost categories. This result should however be seen in the context of high values of SOCC compared to the global average.

Despite the fact that no permafrost category shows a significant difference the amount of SOCC is still large. For a warming of 1.5°C the GDD5 predicts a loss of 4.4 Mio. km^2 (~7.8% loss of total area), which falls into the confidence interval of the predicted values of MAAT by Chadburn et al. (2017) The result for the GDD0 shows a loss of 5.6 Mio. km^2 (~10.0% loss of area). While GDD0 slightly underestimates the loss in area it lies closer to the suggested value by Chadburn et al. (2017) than GDD5, which overestimates the area loss. For obtaining more precise model results of loss in permafrost areas, monitoring efforts and networks should continue to be strongly supported and financed.

7. References

Aalto, J., S. Harrison, and M. Luoto. 2017. Statistical modelling predicts almost complete loss of major periglacial processes in Northern Europe by. *Nature Communications* 8. Springer US: 1–8. doi:10.1038/s41467-017-00669-3.

Åkerman, H. J., and M. Johansson. 2008. Remote sensing of rermafrost-related problems and hazards. *Permafrost and Periglacial Processes* 19 (3): 279–292. doi:10.1002/ppp.

Anisimov, O. A. 2007. Potential feedback of thawing permafrost to the global climate system through methane emission. *Environmental Research Letters* 2. doi:10.1088/1748-9326/2/4/045016.

Anisimov, O. A., and F. E. Nelson. 1996. Permafrost distribution in the northern hemisphere under scenarios of climatic change. *Global and Planetary Change* 14: 59–72. doi:10.1016/0921-8181(96)00002-1.

Anisimov, O. A., and S. Reneva. 2006. Permafrost and Changing Climate : The Russian Perspective 35: 169–175.

Beniston, M., D. Farinotti, M. Stoffel, L. M. Andreassen, E. Coppola, and N. Eckert. 2018. The European mountain cryosphere: a review of its current state, trends, and future challenges: 759–794. doi:10.5194/tc-12-759-2018.

Bockheim, J., G. Vieira, M. Ramos, J. López-Martínez, E. Serrano, M. Guglielmin, K. Wilhelm, and A. Nieuwendam. 2013. Climate warming and permafrost dynamics in the Antarctic Peninsula region. *Global and Planetary Change* 100. Elsevier B.V.: 215–223. doi:10.1016/j.gloplacha.2012.10.018.

Boeckli, L., A. Brenning, S. Gruber, and J. Noetzli. 2012. A statistical approach to modelling permafrost distribution in the European Alps or similar mountain ranges. *Cryosphere* 6: 125–140. doi:10.5194/tc-6-125-2012.

Bolin Centre of Climate of Research, Bolin Centre Database, The Northern Circumpolar Soil Carbon Database. Gridded data in network common data form (NetCDF-files). 2018. Retrieved 13.04.2018, from https://bolin.su.se/data/ncscd/netcdf.php.

Bommer, C., M. Phillips, H.-R. Keusen, and P. Teysseire. 2009. *Bauen im Permafrost*. Birmensdorf: Eidg. Forschungsanstalt für Wald, Schnee und Landschaft WSL.

Brown, J., O. J. Ferrians, J. a. Heginbottom, and E. S. Melnikov. 1997. Brown J. 1997 Circum-Arctic map of permafrost and ground-ice conditions.pdf. *Circum-pacific map series*.

Callaghan, T. V., M. Johansson, R. D. Brown, P. Y. Groisman, N. Labba, V. Radionov, R. S. Bradley, S. Blangy, et al. 2011. Multiple effects of changes in arctic snow cover. *Ambio* 40: 32–45. doi:10.1007/s13280-011-0213-x.

CBC, Randi Beers. Thawing permafrost causes $51M in damages every year to N.W.T. public infrastructure: study. 2017. Retrieved 25.04.2018, from http://www.cbc.ca/news/canada/north/thawing-permafrost-causes-51m-in-damages-every-year-to-n-w-t-public-infrastructure-study-1.4408395.

Chadburn, S. E., E. J. Burke, P. M. Cox, P. Friedlingstein, G. Hugelius, and S. Westermann. 2017. An observation-based constraint on permafrost loss as a function of global warming. *Nature Climate Change* 7: 340–344. doi:10.1038/nclimate3262.

Collins, M., R. Knutti, J. Arblaster, J.-L. Dufresne, T. Fichefet, P. Friedlingstein, X. Gao, W. J. Gutowski, et al. 2013. Long-term Climate Change: Projections, Commitments and Irreversibility. *Climate Change 2013: The Physical Science Basis. Contribution of Working Group I to the Fifth Assessment Report of the Intergovernmental Panel on Climate Change*: 1029–1136. doi:10.1017/CBO9781107415324.024.

Cropwatch, University of Nebraska - Lincoln, Elmore, R. and N. Mueller. Growing degree days and Corn Emergence. 2015. Retrieved 21.05.2018, from https://cropwatch.unl.edu/growing-degree-units-and-corn-emergence.

Dataguru. 2018. Retrieved 06.04.2018, from ftp://dataguru.lu.se/output/68c_wfdei_Tair_19790101_19901231_1day_mean.nc.

Derksen, C., S. L. Smith, M. Sharp, L. Brown, S. Howell, L. Copland, D. R. Mueller, Y. Gauthier, et al. 2012. Variability and change in the Canadian cryosphere. *Climatic Change* 115: 59–88. doi:10.1007/s10584-012-0470-0.

Donnell, J. A. O., N. P. Service, M. T. Jorgenson, V. Romanovsky, J. Harden, Y. Shur, J. O. Donnell, E. A. G. Schuur, et al. 2010. Resilience and Vulnerability of Permafrost to Climate Change climate change 1. doi:10.1139/X10-060.

Etzelmüller, B., E. S. Flo Heggem, N. Sharkhuu, R. Frauenfelder, A. Kääb, and C. Goulden. 2006. Mountain permafrost distribution modelling using a multi-criteria approach in the Hövsgöl area, Northern Mongolia. *Permafrost and Periglacial Processes* 17: 91–104. doi:10.1002/ppp.554.

Van Everdingen, R. 2005. Multi-language glossary of permafrost and related ground-ice terms. *National Snow and Ice Data Center/World Data Center for Glaciology, Boulder* 1998: 186pp. doi:10.2307/1551636.

Frauenfeld, O. W. 2004. Interdecadal changes in seasonal freeze and thaw depths in Russia. *Journal of Geophysical Research* 109: D05101. doi:10.1029/2003JD004245.

Frauenfeld, O. W., T. J. Zhang, and J. L. McCreight. 2007a. Northern hemisphere freezing/thawing index variations over the twentieth century. *Encyclopedia of Atmospheric Sciences* 27: 1549–1555. doi:10.1002/joc.

Frauenfeld, O. W., T. Zhang, and J. L. McCreight. 2007b. Northern hemisphere freezing/thawing index variations over the twentieth century. *International Journal of Climatology* 4: 47–63. doi:10.1002/joc.

Government of the North West Territories, I. Holubec Consulting Inc. Geotechnical site investigation guidelines for building foundations in permafrost. 2010. Retrieved 01.05.2018, from https://www.inf.gov.nt.ca/sites/inf/files/geotechnical_site_investigation_guidelines_for_building_foundations_in_permafrost.pdf.

Government of Saskatchewan, Publications Saskatchewan, Miller, S. and D. Risula. Crop Production News – USING GROWING DEGREE DAYS TO ESTIMATE MATURITY. 2013. Retrieved 23.05.2018, from http://publications.gov.sk.ca/documents/20/83921-ed7ee6a8-5530-416e-8a99-d2e2761560d9.pdf.

Gruber, S. 2012. Derivation and analysis of a high-resolution estimate of global permafrost zonation. *Cryosphere* 6: 221–233. doi:10.5194/tc-6-221-2012.

Gruber, S., and W. Haeberli. 2009. Permafrost Soils 16: 33–44. doi:10.1007/978-3-540-69371-0.

Gruber, S., and M. Hoelzle. 2008. Statistical Modelling ofMountain Permafrost Distribution: Local Calibration and Incorporation of Remotely Sensed Data. *Permafrost and Periglacial Processes* 12: 69–77. doi:10.1002/ppp.

Harris, C., L. U. Arenson, H. H. Christiansen, B. Etzelmüller, R. Frauenfelder, S. Gruber, W. Haeberli, C. Hauck, et al. 2009. Permafrost and climate in Europe: Monitoring and modelling thermal, geomorphological and geotechnical responses. *Earth-Science Reviews* 92. Elsevier B.V.: 117–171. doi:10.1016/j.earscirev.2008.12.002.

Harsch, M. A., P. E. Hulme, M. S. McGlone, and R. P. Duncan. 2009. Are treelines advancing? A global meta-analysis of treeline response to climate warming. *Ecology Letters* 12: 1040–1049.

doi:10.1111/j.1461-0248.2009.01355.x.

Hodgkins, S. B., M. M. Tfaily, C. K. McCalley, T. A. Logan, P. M. Crill, S. R. Saleska, V. I. Rich, and J. P. Chanton. 2014. Changes in peat chemistry associated with permafrost thaw increase greenhouse gas production. *Proceedings of the National Academy of Sciences* 111: 5819–5824. doi:10.1073/pnas.1314641111.

Hoelzle, M., C. Mittaz, and B. Etzelm. 2001. Surface Energy Fluxes and Distribution Models of Permafrost in European Mountain Areas : an Overview of Current Developments 68: 53–68. doi:10.1002/ppp.

IPA. Circumpolar Active Layer Monitoring Network (CALM). 2018. Retrieved 21.05.2018, from https://ipa.arcticportal.org/activities/gtn-p/calm/16-calm.

Johansson, M., T. V. Callaghan, J. Bosiö, H. J. Åkerman, M. Jackowicz-Korczynski, and T. R. Christensen. 2013. Rapid responses of permafrost and vegetation to experimentally increased snow cover in sub-arctic Sweden. *Environmental Research Letters* 8. doi:10.1088/1748-9326/8/3/035025.

Jorgenson, M. T., C. H. Racine, J. C. Walters, and T. E. Osterkamp. 2001. Permafrost degradation and ecological changes associated with a warming climate in central Alaska. *Climatic Change* 48: 551–579. doi:10.1023/A:1005667424292.

Koven, C. D., W. J. Riley, and A. Stern. 2013. Analysis of permafrost thermal dynamics and response to climate change in the CMIP5 earth system models. *Journal of Climate* 26: 1877–1900. doi:10.1175/JCLI-D-12-00228.1.

Mann, M. E., and J. Park. 1996. Greenhouse warning and changes in the seasonal cycle of temperature: model versus observations. *Geophysical Research Letters* 23: 1111–1114. doi:10.1029/96GL01066.

Michigan State University Extension, Battel, B. Understanding growing degree days. 2017. Retrieved 21.5.2018 from http://msue.anr.msu.edu/news/understanding_growing_degree_days.

Natali, S. M., E. A. G. Schuur, and R. L. Rubin. 2012. Increased plant productivity in Alaskan tundra as a result of experimental warming of soil and permafrost. *Journal of Ecology* 100: 488–498. doi:10.1111/j.1365-2745.2011.01925.x.

National Research Council Canada. Division of Building Research. Williams, G. P., and L. W. Gold. 1976. Ground Temperatures. Retrieved 27.03.2018, from http://nparc.nrc-cnrc.gc.ca/eng/view/accepted/?id=386ddf88-fe8d-45dd-aabb-0a55be826f3f.

Nelson, F. E., and S. I. Outcalt. 1987. A Computational Method for Prediction and Regionalization of Permafrost. *Arctic and Alpine Research* 19: 279–288.

Nelson, F. E., O. A. Anisimov, and N. I. Shiklomanov. 2002. Climate change and hazard zonation in the circum-arctic permafrost regions. *Natural Hazards* 26: 203–225. doi:10.1023/A:1015612918401.

Nicolsky, D. J., V. E. Romanovsky, and G. G. Panteleev. 2009. Estimation of soil thermal properties using in-situ temperature measurements in the active layer and permafrost. *Cold Regions Science and Technology* 55. Elsevier B.V.: 120–129. doi:10.1016/j.coldregions.2008.03.003.

NSIDC. Cryosphere Glossary. 2018. Retrieved 23.04.2018, from http://nsidc.org/cryosphere/glossary/P.

Osterkamp, T., and C. Burn. 2015. CRYOSPHERE | Permafrost. In T. Osterkamp, and C. Burn, *Encyclopedia of Atmospheric Sciences* (pp. 208-216). Elsevier.

Osterkamp, T. E. 2005. The recent warming of permafrost in Alaska. *Global and Planetary Change* 49: 187–202. doi:10.1016/j.gloplacha.2005.09.001.

Osterkamp, T. E., and C. R. Burn. 1998. Permafrost: 1717–1729. doi:10.1533/9781855738584.references.

Osterkamp, T. E., and V. E. Romanovsky. 1997. Freezing of the Active Layer on the Coastal Plain of the

Alaskan Arctic. *Permafrost and Periglacial Processes* 8: 23–44. doi:10.1002/(SICI)1099-1530(199701)8:1<23::AID-PPP239>3.0.CO;2-2.

Pangea. 2017. Retrieved 26.03.2018, from https://doi.pangaea.de/10.1594/PANGAEA.873192, Brown, J., Original: Ferrians, O. J. Jr,Heginbottom, J. &Melnikov, E. Circum-ArcticMap of Permafrost and Ground Ice Conditions (National Snow and Ice Data Center, 1998).

Pearson, R. G., S. J. Phillips, M. M. Loranty, P. S. A. Beck, T. Damoulas, S. J. Knight, and S. J. Goetz. 2013. Shifts in Arctic vegetation and associated feedbacks under climate change. *Nature Climate Change* 3. Nature Publishing Group: 673–677. doi:10.1038/nclimate1858.

Popova, V. V., and A. B. Shmakin. 2009. The Influence of Seasonal Climatic Parameters on the Permafrost Thermal Regime, West Siberia, Russia. *Permafrost and Periglacial Processes* 20: 107–136. doi:10.1002/ppp.

Ridefelt, H., B. Etzelmüller, J. Boelhouwers, and C. Jonasson. 2008. Statistic-empirical modelling of mountain permafrost distribution in the Abisko region, sub-Arctic northern Sweden. *Norsk Geografisk Tidsskrift* 62: 278–289. doi:10.1080/00291950802517890.

Riseborough, D. W., et al., N. I. Shiklomanov, B. Etzelmüller, S. Gruber, and S. Marchenko. 2008. Recent Advances in Permafrost Modelling. *Permafrost and Periglacial Processes* 19: 137–156. doi:10.1002/ppp.

Schuur, E., J. Bockheim, and J. Canadell. 2008. Vulnerability of permafrost carbon to climate change: Implications for the global carbon cycle. … 58: 701. doi:10.1641/B580807.

Schuur, E. A. G., B. W. Abbott, W. B. Bowden, V. Brovkin, P. Camill, J. G. Canadell, J. P. Chanton, F. S. Chapin, et al. 2013. Expert assessment of vulnerability of permafrost carbon to climate change. *Climatic Change* 119: 359–374. doi:10.1007/s10584-013-0730-7.

Schuur, E. A. G., A. D. McGuire, C. Schädel, G. Grosse, J. W. Harden, D. J. Hayes, G. Hugelius, C. D. Koven, et al. 2015. Climate change and the permafrost carbon feedback. *Nature* 520: 171–179. doi:10.1038/nature14338.

Schweizerischer Verband der Strassen- und Verkehrsfachleute (VSS). 2001. *Schweizer Norm 670140b, Frost*. Edited by VSS Fachkokmission 5. Zürich: Schweizerischer Verband der Strassen- und Verkehrsfachleute (VSS).

Serreze, M. C., J. E. Walsh, F. S. I. Chapin, T. Osterkamp, M. Dyurgerov, V. Romanovsky, W. C. Oechel, J. Morison, et al. 2000. Observational evidence of recent change in the northern high-latitude environment. *Climatic Change* 46: 159–207. doi:10.1023/A:1005504031923.

Serreze, M. C., A. P. Barrett, J. C. Stroeve, D. N. Kindig, and M. M. Holland. 2009. The emergence of surface-based Arctic amplification. *Cryosphere* 3: 11–19. doi:10.5194/tc-3-11-2009.

Shi, Y., F. Niu, C. Yang, T. Che, Z. Lin, and J. Luo. 2018. Permafrost presence/absence mapping of the Qinghai-Tibet Plateau based on multi-source remote sensing data. *Remote Sensing* 10. doi:10.3390/rs10020309.

Shiklomanov, N. I., and F. E. Nelson. 2013. Thermokarst and Civil Infrastructure. *Treatise on Geomorphology* 8: 354–373. doi:10.1016/B978-0-12-374739-6.00214-1.

Shur, Y. L., and M. T. Jorgenson. 2007. Patterns of Permafrost Formation and Degradation in Relation to Climate and Ecosystems 19: 7–19. doi:10.1002/ppp.

Slater, A. G., and D. M. Lawrence. 2013. Diagnosing present and future permafrost from climate models. *Journal of Climate* 26: 5608–5623. doi:10.1175/JCLI-D-12-00341.1.

Smith, M., and D. Riseborough. 1998. Short communication: Permafrost monitoring and detection of climate change—a reply. *Permafrost and Periglacial Processes* 9: 91–92. doi:CCC 1045-6740/98/010091.

Smith, M. W., and D. W. Riseborough. 1996. Permafrost monitoring and detection of climate change. *Permafrost and Periglacial Processes* 7: 301–309. doi:10.1002/(SICI)1099-1530(199610)7:4<301::AID-PPP231>3.0.CO;2-R.

Smith, M. W., and D. W. Riseborough. 2002. Climate and the limits of permafrost: A zonal analysis. *Permafrost and Periglacial Processes* 13: 1–15. doi:10.1002/ppp.410.

Smith, S., and J. Brown. 2009. Essential Climate Variables: Permafrost and seasonally frozen ground: 22.

Smith, S. L., V. E. Romanovsky, A. G. Lewkowicz, C. R. Burn, M. Allard, G. D. Clow, K. Yoshikawa, and J. Throop. 2010. Thermal state of permafrost in North America: A contribution to the international polar year. *Permafrost and Periglacial Processes* 21: 117–135. doi:10.1002/ppp.690.

Stieglitz, M., S. J. Déry, V. E. Romanovsky, and T. E. Osterkamp. 2003. The role of snow cover in the warming of arctic permafrost. *Geophysical Research Letters* 30: 1–4. doi:10.1029/2003GL017337.

Tarnocai, C., J. G. Canadell, E. A. G. Schuur, P. Kuhry, G. Mazhitova, and S. Zimov. 2009. Soil organic carbon pools in the northern circumpolar permafrost region. *Global Biogeochemical Cycles* 23: 1–11. doi:10.1029/2008GB003327.

Waller, R. I., J. B. Murton, and L. Kristensen. 2012. Glacier-permafrost interactions: Processes, products and glaciological implications. *Sedimentary Geology* 255–256. Elsevier B.V.: 1–28. doi:10.1016/j.sedgeo.2012.02.005.

Walvoord, M. A., and B. L. Kurylyk. 2016. Hydrologic Impacts of Thawing Permafrost—A Review. *Vadose Zone Journal* 15: 0. doi:10.2136/vzj2016.01.0010.

Wang, W., A. Rinke, J. C. Moore, D. Ji, X. Cui, S. Peng, D. M. Lawrence, A. D. McGuire, et al. 2016. Evaluation of air-soil temperature relationships simulated by land surface models during winter across the permafrost region. *Cryosphere* 10: 1721–1737. doi:10.5194/tc-10-1721-2016.

Woo, M. K. 2012. *Permafrost Hydrology*. Heidelberg, Dordrecht, London, New York: Springer.

Worldclim. Bioclimatic variables. 2017. Retrieved 06.04.2018, from http://worldclim.org/bioclim.

Wu, T., Q. Wang, L. Zhao, O. Batkhishig, and M. Watanabe. 2011. Observed trends in surface freezing/thawing index over the period 1987-2005 in Mongolia. *Cold Regions Science and Technology* 69. Elsevier B.V.: 105–111. doi:10.1016/j.coldregions.2011.07.003.

Xu, L., R. B. Myneni, F. S. Chapin, T. V. Callaghan, J. E. Pinzon, C. J. Tucker, Z. Zhu, J. Bi, et al. 2013. Temperature and vegetation seasonality diminishment over northern lands. *Nature Climate Change* 3: 581–586. doi:10.1038/nclimate1836.

Xu, T., and M. Hutchinson. 2011. ANUCLIM version 6.1 user guide. *The Australian National University, FennerSchool of Environment and Society, Canberra.*: 90p.

Zhang, T. 2005. Influence of seasonal snow cover on the ground thermal regime: an overview. *Reviews in Geophysics* 43: RG4002. doi:10.1029/2004RG000157.1.INTRODUCTION.

Zhang, T., R. G. Barry, K. Knowles, J. A. Heginbottom, and J. Brown. 2008. Statistics and characteristics of permafrost and ground-ice distribution in the Northern Hemisphere. *Polar Geography* 31: 47–68. doi:10.1080/10889370802175895.

Zhang, W., P. A. Miller, B. Smith, R. Wania, T. Koenigk, and R. D??scher. 2013. Tundra shrubification and tree-line advance amplify arctic climate warming: Results from an individual-based dynamic vegetation model. *Environmental Research Letters* 8. doi:10.1088/1748-9326/8/3/034023.

8. Appendix

Table 1: Statistics of all variables in continuous permafrost.

	lon	lat	pfrac	seasonality	SOCC	GDD5	GDD0	FDD	MAAT
nbr.val	12380.00	12380.00	12380.00	12380.00	12380.00	12380.00	12380.00	12380.00	12380.00
nbr.null	0.00	0.00	0.00	11.00	2480.00	3005.00	1757.00	0.00	0.00
nbr.na	0.00	0.00	0.00	0.00	0.00	0.00	0.00	0.00	0.00
min	-179.75	46.75	0.90	0.00	0.00	0.00	0.00	2448.45	245.32
max	179.75	83.25	1.00	2381.44	2099.00	1154.68	1864.93	10184.19	267.95
range	359.50	36.50	0.10	2381.44	2099.00	1154.68	1864.93	7735.74	22.62
sum	211295.50	852355.50	12308.23	18146989.15	6874677.00	3725707.24	8529300.77	69655926.82	3214584.36
median	-23.25	68.25	1.00	1490.55	615.00	243.99	726.63	5452.76	260.40
mean	17.07	68.85	0.99	1465.83	555.31	300.95	688.96	5626.49	259.66
SE.mean	0.95	0.06	0.00	3.09	3.50	2.66	4.53	13.82	0.05
CI.mean.0.95	1.87	0.12	0.00	6.06	6.86	5.21	8.88	27.09	0.09
var	11239.50	44.20	0.00	118279.37	151470.25	87446.60	254040.34	2364153.17	25.77
std.dev	106.02	6.65	0.02	343.92	389.19	295.71	504.02	1537.58	5.08
coef.var	6.21	0.10	0.02	0.23	0.70	0.98	0.73	0.27	0.02

Table 2: Statistics of all variables in discontinuous permafrost.

	lon	lat	pfrac	seasonality	SOCC	GDD5	GDD0	FDD	MAAT
nbr.val	1987.00	1987.00	1987.00	1987.00	1987.00	1987.00	1987.00	1987.00	1987.00
nbr.null	0.00	0.00	0.00	0.00	83.00	32.00	0.00	0.00	0.00
nbr.na	0.00	0.00	0.00	0.00	0.00	0.00	0.00	0.00	0.00
min	-175.75	46.25	0.50	358.37	0.00	0.00	57.78	1895.51	266.40
max	179.25	79.75	0.91	1905.30	2506.00	1343.14	2135.85	4092.09	269.52
range	355.00	33.50	0.41	1546.94	2506.00	1343.14	2078.08	2196.57	3.12
sum	2917.25	119714.75	1460.83	2700422.30	1191703.00	1338469.04	2651845.44	6374706.50	532577.30
median	60.75	61.25	0.75	1393.37	508.00	691.72	1359.43	3214.29	268.02
mean	1.47	60.25	0.74	1359.04	599.75	673.61	1334.60	3208.21	268.03
SE.mean	2.47	0.12	0.00	5.50	8.69	5.91	7.65	7.80	0.01
CI.mean.0.95	4.85	0.23	0.01	10.79	17.05	11.59	15.00	15.29	0.03
var	12168.28	26.80	0.01	60109.56	150164.32	69366.80	116296.56	120795.45	0.42
std.dev	110.31	5.18	0.12	245.17	387.51	263.38	341.02	347.56	0.65
coef.var	75.13	0.09	0.16	0.18	0.65	0.39	0.26	0.11	0.00

Table 3: Statistics of all variables in sporadic permafrost.

	lon	lat	pfrac	seasonality	SOCC	GDD5	GDD0	FDD	MAAT
nbr.val	1872.00	1872.00	1872.00	1872.00	1872.00	1872.00	1872.00	1872.00	1872.00
nbr.null	0.00	0.00	0.00	0.00	58.00	7.00	0.00	0.00	0.00
nbr.na	0.00	0.00	0.00	0.00	0.00	0.00	0.00	0.00	0.00
min	-170.25	45.75	0.10	347.80	0.00	0.00	219.70	1420.39	268.27
max	166.25	70.25	0.51	1902.04	2653.00	1552.63	2428.58	3605.57	271.45
range	336.50	24.50	0.41	1554.24	2653.00	1552.63	2208.88	2185.17	3.18
sum	-5551.00	109239.00	521.37	2443660.93	1285914.00	1556246.70	2934980.64	5055197.40	505543.86
median	24.75	59.25	0.26	1365.90	539.00	880.18	1629.69	2736.98	270.05
mean	-2.97	58.35	0.28	1305.37	686.92	831.33	1567.83	2700.43	270.06
SE.mean	2.40	0.12	0.00	5.56	11.93	6.45	7.93	8.28	0.01
CI.mean.0.95	4.71	0.24	0.01	10.90	23.40	12.66	15.54	16.24	0.03
var	10805.92	29.06	0.01	57853.22	266582.55	77968.86	117589.52	128405.82	0.37
std.dev	103.95	5.39	0.12	240.53	516.32	279.23	342.91	358.34	0.61
coef.var	-35.06	0.09	0.43	0.18	0.75	0.34	0.22	0.13	0.00

Table 4: Statistics of all variables in isolated permafrost.

	lon	lat	pfrac	seasonality	SOCC	GDD5	GDD0	FDD	MAAT
nbr.val	1807.00	1807.00	1807.00	1807.00	1807.00	1807.00	1807.00	1807.00	1807.00
nbr.null	0.00	0.00	0.00	0.00	77.00	0.00	0.00	0.00	0.00
nbr.na	0.00	0.00	0.00	0.00	0.00	0.00	0.00	0.00	0.00
min	-166.75	43.75	0.00	340.98	0.00	0.79	369.42	29.20	270.35
max	163.75	70.75	0.11	2020.67	3212.00	2545.51	3614.47	3185.92	279.51
range	330.50	27.00	0.11	1679.70	3212.00	2544.72	3245.05	3156.71	9.16
sum	-39636.75	100161.25	59.84	2123939.47	1137128.00	1732280.26	3226601.16	3624650.28	492494.48
median	-60.25	54.75	0.02	1287.78	396.00	1039.89	1868.48	2197.65	272.16
mean	-21.94	55.43	0.03	1175.40	629.29	958.65	1785.61	2005.89	272.55
SE.mean	2.41	0.13	0.00	7.02	13.21	8.26	9.67	14.18	0.03
CI.mean.0.95	4.73	0.26	0.00	13.77	25.91	16.21	18.97	27.80	0.07
var	10507.43	30.92	0.00	89061.98	315459.73	123365.73	168984.39	363089.30	2.13
std.dev	102.51	5.56	0.03	298.43	561.66	351.23	411.08	602.57	1.46
coef.var	-4.67	0.10	0.96	0.25	0.89	0.37	0.23	0.30	0.01

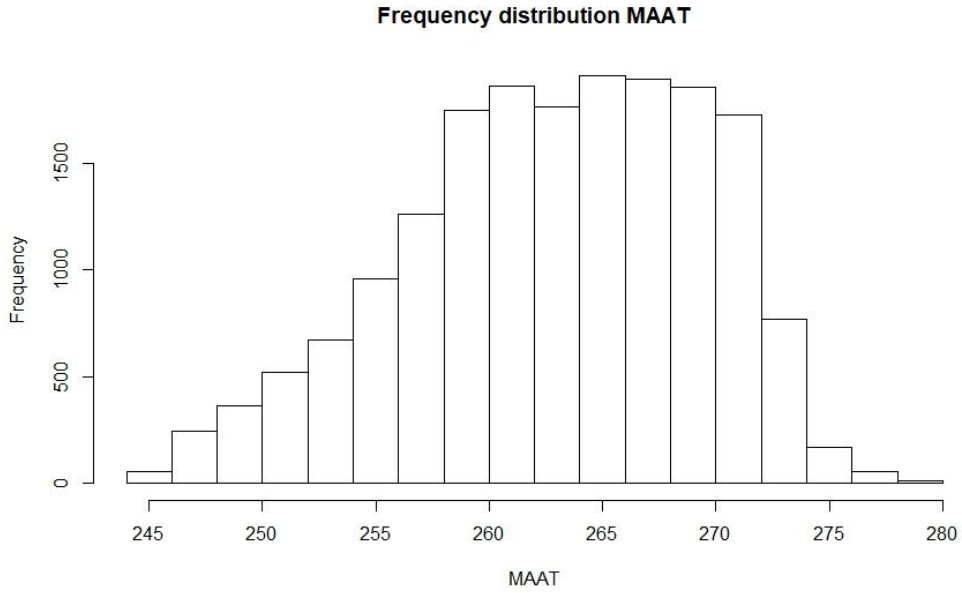

Figure 1: Frequency distribution of MAAT.

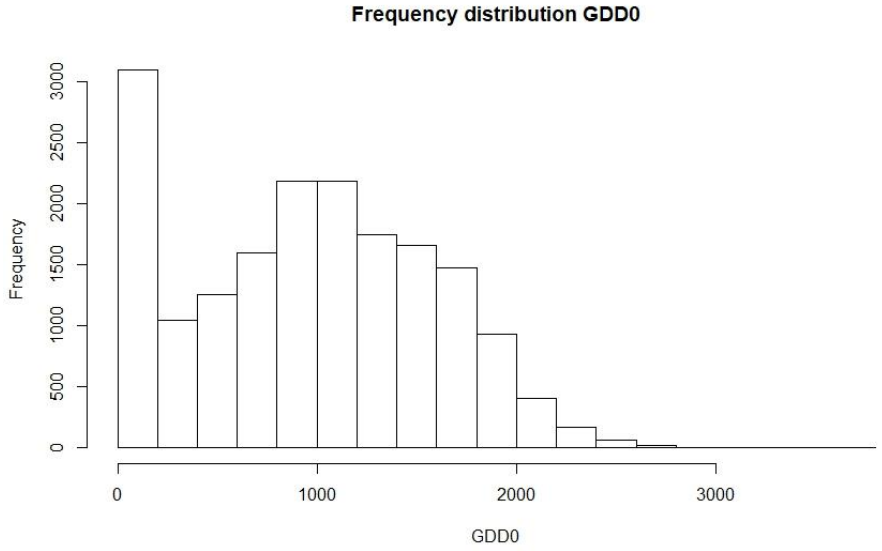

Figure 2: Frequency distribution of GDD0.

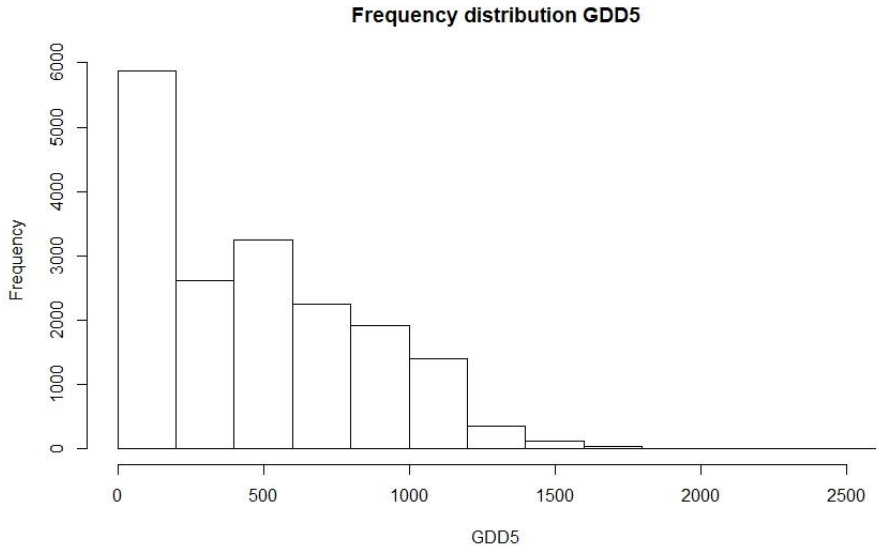

Figure 3: Frequency distribution of GDD5.

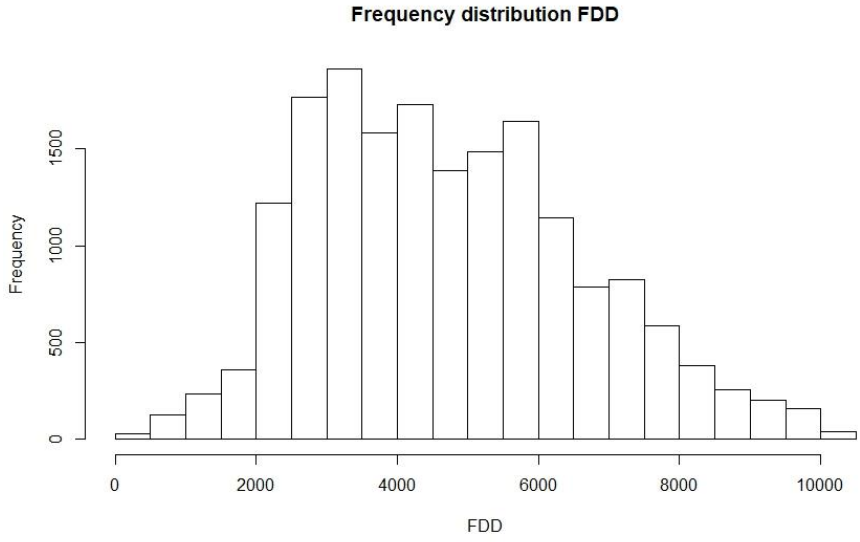

Figure 4: Frequency distribution of FDD.

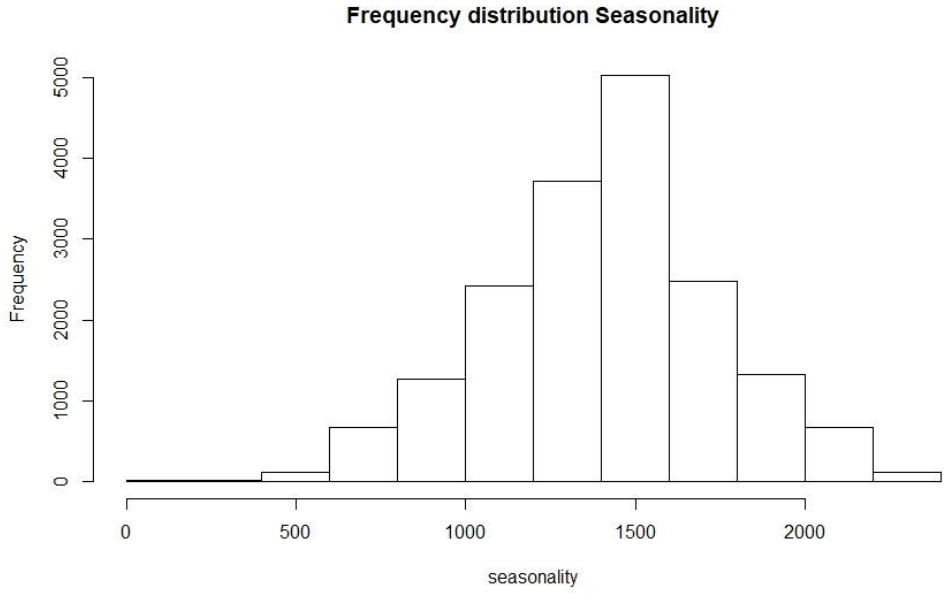

Figure 5: Frequency distribution of seasonality.

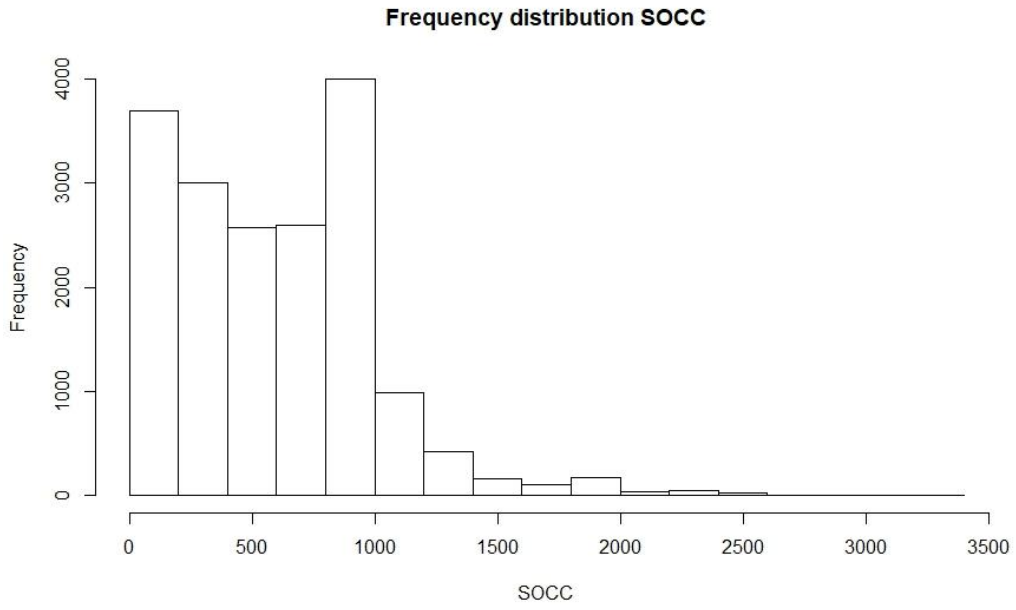

Figure 6: Frequency distribution of SOCC.